ISSN: 1231-4005
e-ISSN: 2354-0133
ICID: 1134108
DOI: 10.5604/12314005.1134108

THE DYNAMICS THE ASSEMBLY INCLUDING LIGHT TRAILER – VEHICLE WITH COMBUSTION ENGINE OR HYBRID DRIVING

Krzysztof Siczek

Lodz University of Technology
Department of Vehicles and Fundamentals of Machine Design
Zeromskiego Street 116, 90-924 Lodz, Poland
tel.: +48 42 6312250, fax: +48 42 6312252
e-mail: ks670907@p.lodz.pl

Krzysztof Wituszyński

Warsaw Management University
Kaweczynska Street 36 03-772 Warsaw, Poland
tel.: +48 607 169 107

Abstract

The rising greenhouse gas emissions at a global level have caused the increasing interest in cleaner and less oil-dependent transportation sources. It has been carried out a lot of researches on the alternative energy sources, like biofuels, fuel cells, wind farms, etc. and on the clean vehicles (hybrids). Most major manufacturers have successfully introduced hybrid automobiles utilizing electric motors and an internal combustion engine to improve their gas mileage. To decrease the use of gasoline even further, some hybrids are being retrofitted to allow them to be plugged-into a standard i.e. 120-volt socket to charge the batteries and potentially to provide power back to the electric grid when needed. Plug-in Hybrid Cars offer the fuel-efficiency benefits of hybrid cars with the added feature of being able to plug-in to household electricity during rest. This allows the increased mileage and fuel savings. Plug-ins requires larger batteries than normal hybrids, which drives up their cost. Lithium-ion batteries are smaller, have a higher output of energy but are more expensive than rechargeable nickel metal hydride (NiMh), still used in hybrid vehicles. Improvement in battery storage capacity is of the most importance for the plug-ins. Plug-in technology is developed by the major auto manufacturers, with working prototypes of both plug-in hybrid electric vehicles (PHEV) and plug-in electric vehicles possessing small backup gas generators. The aim of the paper has been to assess the dynamic performance characteristics of the assembly light trailer – car with classic combustion engine (in the first case) or PHEV (in the second case), using mathematical models and numerical simulations of standard driving cycles and to investigate algorithms for charging the stock battery pack.

Keywords: *combustion engine, plug-in hybrid electric vehicle, light trailer, dynamics*

1. Introduction

The rising greenhouse gas emissions at a global level have caused the increasing interest in cleaner and less oil-dependent transportation sources. It has been carried out a lot of researches on the alternative energy sources, like biofuels, fuel cells, wind farms, etc. and on the clean vehicles (hybrids). Most major manufacturers have successfully introduced hybrid automobiles utilizing electric motors and an internal combustion engine to improve their gas mileage. To decrease the use of gasoline even further, some hybrids are being retrofitted to allow them to be plugged-into a standard i.e. 120-volt socket to charge the batteries and potentially to provide power back to the electric grid when needed.

In 2010, a hybrid Toyota Prius (hybrid electric vehicle – HEV) is being retrofitted into an experimental plug-in hybrid electric vehicle (PHEV). For the conversion, a secondary battery pack was installed to be charged via a standard 120-volt wall socket. The secondary battery can

recharge the Prius stock battery during vehicle operation to minimize the usage of the internal combustion engine (ICE). The aim of the paper has been to assess the dynamic performance characteristics of PHEVs using mathematical models and numerical simulations of standard driving cycles and to investigate algorithms for charging the stock battery pack.

2. Vehicle – lightweight trailer set

The considered model of the set vehicle – trailer has been shown in the Fig. 1. In the model it has been omitted the resistance of air acting on the trailer. The lightweight trailer weight M_p can be equal up to 750 kg. For the further analysis, it has been assumed, that such weight is equal its maximum value. For the simplicity of calculations it has been assumed that the forces P_p (resistance of air), P_b, (vehicle inertia force), P_{bp} (trailer inertia force) and $P_n = F_{res}$ (total resistance force) act in the same high, described by variable $z = \left(d + h_c + h_{cp}\right)/3$.

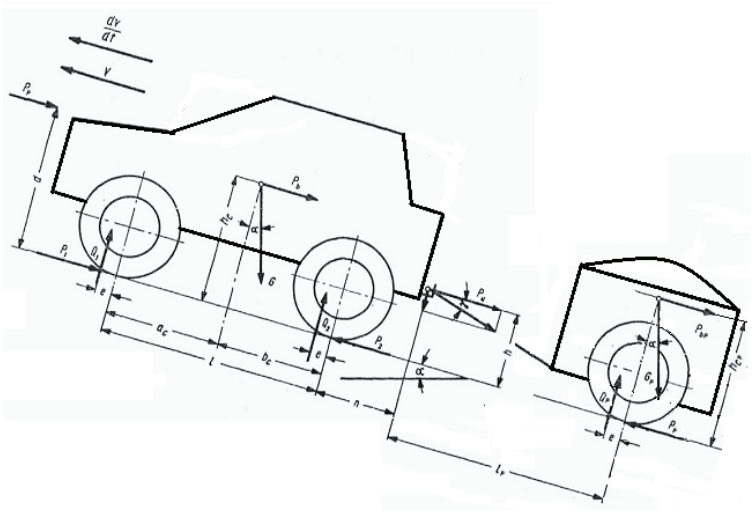

Fig. 1. The model of the set vehicle – trailer

The reaction acting on the wheel of the vehicle (Q_1, Q_2) and of the trailer (Q_p) can be obtained from the equations (1) – (4).

$$Q_1 = \left[G\left(\left(b_c - f_R r_d\right)\cos\alpha - h_c \sin\alpha\right) - 0.0048 c_x F V^2 d - G g^{-1} \dot{V} h_c - P_u\left(h + \left(n + f_R R_w\right) tg\gamma\right)\right] \cdot l^{-1}$$
$$\approx \left[G b_c \cos\alpha - P_n z\right] \cdot l^{-1}, \tag{1}$$

$$Q_2 = \left[G\left(\left(a_c + f_R r_d\right)\cos\alpha + h_c \sin\alpha\right) + 0.0048 c_x F V^2 d + G g^{-1} \dot{V} h_c + P_u\left(h + \left(l + n + f_R R_w\right) tg\gamma\right)\right] \cdot l^{-1}$$
$$\approx \left[G a_c \cos\alpha + P_n z\right] \cdot l^{-1}, \tag{2}$$

$$P_n = f_R G \cos\alpha + G \sin\alpha + 0.0048 C_x S V^2 + \left(G g^{-1} + 2 J_k R_w^{-2}\right)\dot{V} + P_u, \tag{3}$$

$$Q_p \approx G_p \cos\alpha. \tag{4}$$

3. Series parallel vehicle

It has been analysed two cases of vehicle:

- one operating only with the same engine as in the case of Toyota Prius,
- one of the series parallel types, like Toyota Prius, with its innovative power-split power train.

Such vehicle is the more and more popular hybrid electric one, because of its interesting properties. Its power-split power train is the most efficient one, comparing to parallel hybrid, series

hybrid, stop/start and conventional power trains, all designed for the same vehicle specifications and performances [1].

The advantage of its power-split power train is due to the eCVT transmission system, where the additional benefit comparing to the other parallel and series hybrid power trains comes from:

- the optimized control of the engine operations decoupled from the wheels speed,
- the electric drive mode avoiding low efficiency engine operations at low velocity driving,
- the brake energy recovery during decelerations due to high power electric generator implemented and bigger battery capacity [1].

The schematic view of the vehicle can be seen in Fig. 2 [2].

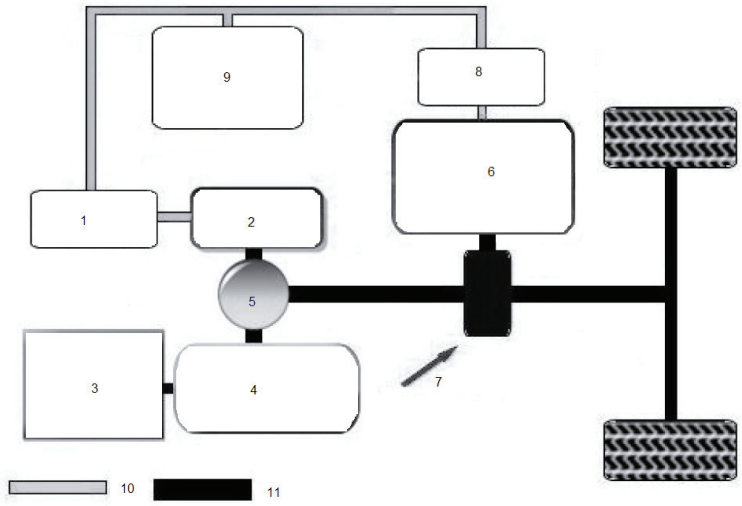

Fig. 2. Serial – Parallel HEV; 1 – PE Convertor, 2 – Generator, 3 – Fuel tank, 4 – ICE, 5 – Power Split Device, 6 – Motor Generator, 7 – Transmission, 8 – PE Convertor, 9 – Battery Pack 10 – Electrical connection, 11 – Mechanical connection, based on [2]

The motion of the set vehicle – trailer can be calculated using the equations (5) – during acceleration or constant velocity or (6) during deceleration. The force P_u can be calculated from the equation (7).

$$K_D R_W^{-1}\left(\left(1-k_b\right)^{-1}\cdot\eta_{FGT}\cdot C_{ICE}+C_{MG2}\right)-\left(Mgf_R+0.5\rho C_x S V^2+Mg\sin\alpha+P_u\right)=M\dot{V}\,, \tag{5}$$

$$-F_B-K_D R_W^{-1}C_{MG2}-\left(Mgf_R+0.5\rho C_x S V^2+Mg\sin\alpha+P_u\right)=kM\dot{V}\,, \tag{6}$$

$$P_u=M_p g f_R+M_p g\sin\alpha+M_p\dot{V}\,, \tag{7}$$

where:

F_B – hydraulic braking forces,
k =1.1 – the rotational inertia coefficient to compensate for the apparent increase in the Prius' mass due to rotating mass, a – acceleration [m/s^2],
C – torque [Nm],
C_X = 0.254 – drag coefficient [-],
F – force [N],
f_R =0.015 – rolling resistance coefficient [-],
g = 9.81 – gravitational acceleration [m/s^2],
J – inertia [kg.m^2],
k_b = -1/2.6 – basic velocity ratio of PGT [-],
M = 1725 – vehicle weight [kg],
M_p = 750 [kg] – trailer weight,

P – power [kW],
$R_W = 0.3$ – wheel radius [m],
S – surface [m^2],
V – velocity [km/h],
η – efficiency [-],
$\rho = 1.12$ – air density [kg/m^3],
α – road grade [°],
ω – speed [rpm].

When the weight of trailer is equal, the equations (1) and (2) become the same as in the [2].

The modelling of the THS-II power train considered for this study is fully detailed in [2, 3].

Matrix equation governing the series/parallel operation of the eCVT function of the power train is of the form (8).

$$\begin{bmatrix} 1 & (1-k_b)k_b^{-1} & 0 \\ 1 & 0 & 1-k_b \end{bmatrix} \begin{bmatrix} C_{ICE} \\ C_{MG1} \\ C_{MG2} \end{bmatrix} = \begin{bmatrix} \alpha & \beta \\ \gamma & \delta \end{bmatrix} \begin{bmatrix} \dot{\omega}_{ICE} \\ \dot{\omega}_{MG2} \end{bmatrix} + \begin{bmatrix} 0 \\ (1-k_b)K_D^{-1}R_W(F_{res}+F_B) \end{bmatrix}, \tag{8}$$

where:

$$\alpha = (1-k_b)^2 k_b^{-2}(J_{MG1}+J_S)+(J_{ICE}+J_{PC}); \beta = (1-k_b)k_b^{-2}(J_{MG1}+J_S),$$
$$\gamma = J_{ICE}+J_{PC}; \delta = (1-k_b)k_D^{-2}(MR_W^2+J_W+J_a)+(1-k_b)(J_{MG2}+J_R),$$
$$F_{res} = f_R G\cos\alpha + G\sin\alpha + 0.0048C_x SV^2 + (Gg^{-1}+2J_k R_W^{-2})\dot{V} + P_u.$$

The dynamic behaviour of the battery and its power bus is obtained from the equations (9) – (10).

$$P_{batt} = P_{MG1.elec}\cdot\eta_{MEP}^{k} - P_{MG2.elec}\cdot\eta_{MEP}^{-k} = (C_{MG1}\cdot\omega_{MG1}\cdot\eta_{MG1}^{k})\cdot\eta_{MEP}^{k} - (C_{MG2}\cdot\omega_{MG2}\cdot\eta_{MG2}^{-k})\cdot\eta_{MEP}^{-k}, \tag{9}$$

$$E_{batt}(t) = \int P_{batt}\cdot dt, \tag{10}$$

where:

$J_{ICE} = 0.13$ – internal combustion engine inertia [kg.m^2],
$J_{MG1} = 0.0113$ – electric motor/generator inertia [kg.m^2],
$J_{MG2} = 0.0226$ – electric motor/generator 2 inertia [kg.m^2],
$J_S = 0.001$ – sun gear inertia [kg.m^2],
$J_{PC} = 0.001$ – planet carrier gear inertia [kg.m^2],
$J_R = 0.001$ – ring gear inertia [kg.m^2],
$J_a = 0.13$ – a inertia [kg.m^2],
$J_k = 0.71$ – k inertia [kg.m^2],
$K_D = 4.113$ – differential gear ratio.

Similarly to the [3], the state variables of the THS-II power train are the engine speed (ω_{ICE}), the velocity of the vehicle (V, proportional to ω_{MG2}), and the variation of battery energy P_{batt}. The control variables are the torque of the engine (C_{ICE}), of MG1 (C_{MG1}), and MG2 (C_{MG2}). The MG1 refers to the motor generator at the engine side, and MG2 the motor generator in charge of the electric traction mode. Due to the large number of state and control variables, the computation time of algorithm could be too excessive. A simplification of the problem and it solution has been described in [3].

The architecture of THS-II power train model, used in the analysis is shown in the Fig. 3.

The problem is simplified into one control (or independent) variable P_{batt}, over which the minimization will be performed. P_{ICE} is now a dependant variable, thus a state variable that can be determined from P_{batt}. All the other variables describing the operation of the power train become state (or dependant) variables that can be deduced from P_{batt} at each time t with the equations (11) – (20) – for Traction mode ($P_d>0$ demand power), and with (21) – (27) – for Braking mode ($P_d<0$).

It has been assumed, that efficiencies $\eta_{FTG} = \eta_{MG1} = \eta_{MG2} = 0.98$ [-]. It has been also assumed, that analysed hybrid vehicle always operates according its e-line – Economic line. The approximated

engine optimum operating line (e-line) for Toyota Prius has been elaborated basing on the experimental data described in [4] and shown in the Fig. 4.

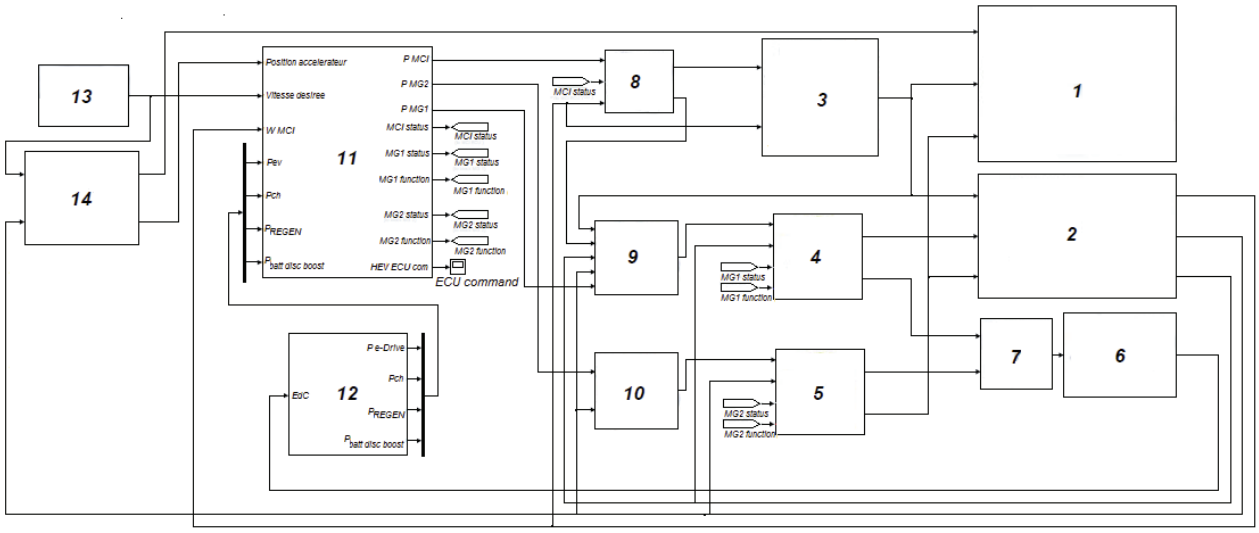

Fig. 3. Overall architecture of THS-II power train model; 1 – vehicle-trailer set, 2 – THS-II power train dynamics, 3 – ICE, 4 – MG1, 5 – MG2, 6 – Battery, 7 – Power bus, 8 – ICE ECU, 9 – MG1 ECU, 10 – MG2 ECU, 11 – HEV ECU, 12 – Battery ECU, 13 – Driving cycle, 14 – Driver

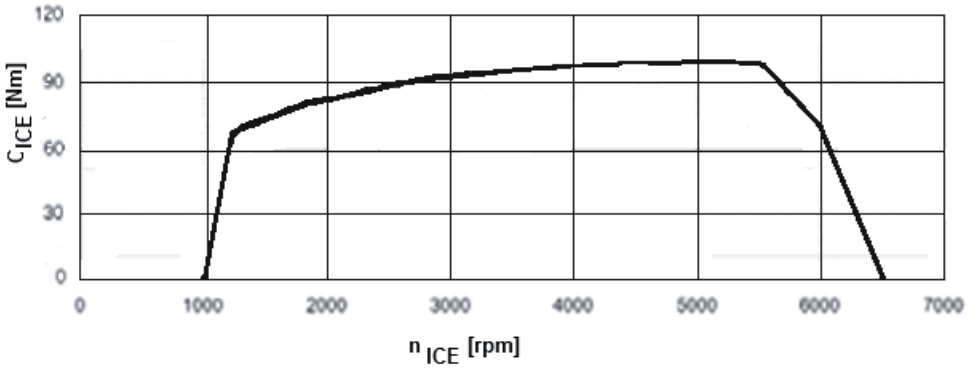

Fig. 4. Approximated engine optimum operating line (e-line) for Toyota Prius

$$\omega_{ICE} = f_{e-line}(P_{ICE}), \tag{11}$$

$$C_{ICE} = P_{ICE} / \omega_{ICE}, \tag{12}$$

$$\omega_{MG2} = K_D R_W^{-1} V, \tag{13}$$

$$\omega_{MG1} = (k_b - 1)k_b^{-1}\omega_{ICE} + k_b^{-1}\omega_{MG2}, \tag{14}$$

$$C_{MG1} = k_b(k_b - 1)^{-1}(C_{ICE} - \alpha\dot{\omega}_{ICE} - \beta\dot{\omega}_{MG2}), \tag{15}$$

$$P_{mechMG1} = C_{MG1}\omega_{MG1}, \tag{16}$$

$$P_{elecMG1} = P_{mechMG1}\eta_{MG1}, \tag{17}$$

$$P_{elecMG2} = -P_{batt} + P_{elecMG1}, \tag{18}$$

$$P_{mechMG2} = P_{elecMG2}\eta_{MG2}, \tag{19}$$

$$C_{MG2} = P_{mechMG2} / \omega_{MG2}, \tag{20}$$

$$P_{mechMG2} = \min\left(C_{recuperation} \times P_d; P_{\min MG2}\right), \tag{21}$$

$$P_{elecMG2} = P_{mechMG2} \cdot \eta_{MG2}, \tag{22}$$

$$\omega_{MG2} = K_D R_W^{-1} V, \tag{23}$$

$$C_{MG2} = P_{mechMG2} / \omega_{MG2}, \tag{24}$$

$$ICE\,OFF : P_{ICE} = 0; C_{ICE} = 0; \omega_{ICE} = 0, \tag{25}$$

$$MG1\,OFF : P_{MG2} = 0; C_{MG2} = 0, \omega_{ICE} = k_b^{-1} \omega_{MG2}, \tag{26}$$

$$P_{batt} = -P_{elecMG2}. \tag{27}$$

The State of Charge for the battery SOC can be calculated from the equation (28).

$$SOC(t) = \left\{C_{\max} - \left[\int (-I/3600)dt + (C_{\max} - C_{ini})\right]\right\} C_{\max}^{-1}, \tag{28}$$

where:
C_{max} – the maximum capacity of the battery,
C_{ini} – initial capacity at the beginning of the simulation,
I – the current supplied by the battery.

The maximum and initial capacities are set at the beginning of the simulation; however, the current is variable, depending on the power received or supplied by the battery during the simulation. During analysis, the values of SOC are as it is shown in the Fig. 5, according to the [4].

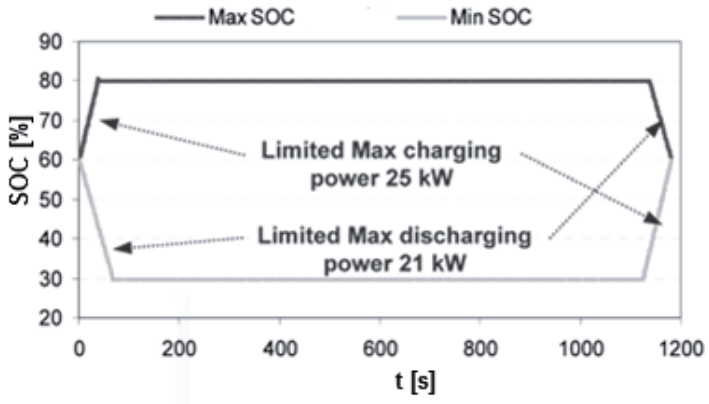

Fig. 5. Limitations of SOC [4]

During analysis, the following constraints (29) have been included for the THS-II power train.

$$\begin{cases} C_{MG2\min} \le C_{MG2} \le C_{MG2\max} = 400Nm; C_{MG1\min} \le C_{MG1} \le C_{MG1\max} = 31Nm; \\ 0 \le \omega_{MG2} \le 600\,RPM; -10000 \le \omega_{MG1} \le 1000RPM; 0 \le C_{ICE} \le C_{ICE\max} = 115Nm; \\ \omega_{ICE\min} \le \omega_{ICE} \le \omega_{ICE\max}; -50 \le P_{MG2} \le 50\,kW; -30 \le P_{MG1} \le 30\,kW; 0 \le P_{ICE} \le 57\,kW. \end{cases} \tag{29}$$

Values of the $\omega_{ICE\min}, \omega_{ICE\max}$ can be determined from the Fig. 6, and depend on the separation factor SF of the THS+II power train, calculated from the equation (30).

$$SF = K_D \cdot R_W^{-1} \cdot (1 - k_b)^{-1} \cdot V \cdot \omega_{ICE}^{-1}. \tag{30}$$

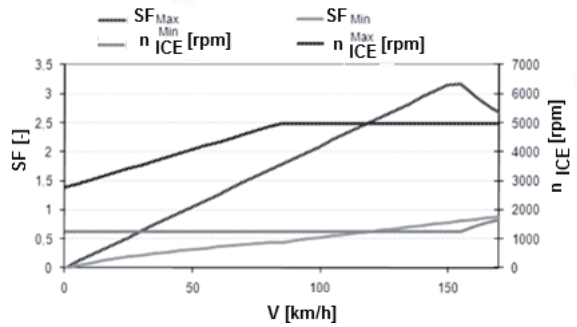

Fig. 6. Separation factor SF and engine speed $\omega_{ICE\,\min}$, $\omega_{ICE\,\max}$ against vehicle speed V [4]

The strategy and control algorithm has been very similar to that described in [3-5].

3. Drive cycle and results of calculations

The calculations of dynamics the assembly including light trailer and vehicle has been carried out using model of standard NUDC drive cycle [5] presented in the Fig. 7.

In all presented further Fig. 8-13, the course 1 is for the vehicle without the trailer, the course 2 is for the case of the vehicle with the trailer.

The obtained courses of P_{ICE} against time t for the case of vehicle operating with classic combustion engine has been presented in the Fig. 8.

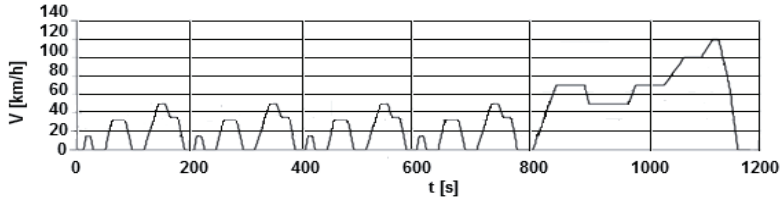

Fig. 7. NUDC drive cycle [6]

For the case of hybrid vehicle, the course of SOC against time t has been presented in the Fig. 9. The power P_{batt} against time t has been shown in the Fig. 10. The power P_{ICE} against time has been presented in the Fig. 11. Both in the case with and without trailer the courses P_{ICE} of are the same. The power P_{MG1} against time t has been shown in the Fig. 12. The power P_{MG2} against time t has been shown in the Fig. 13.

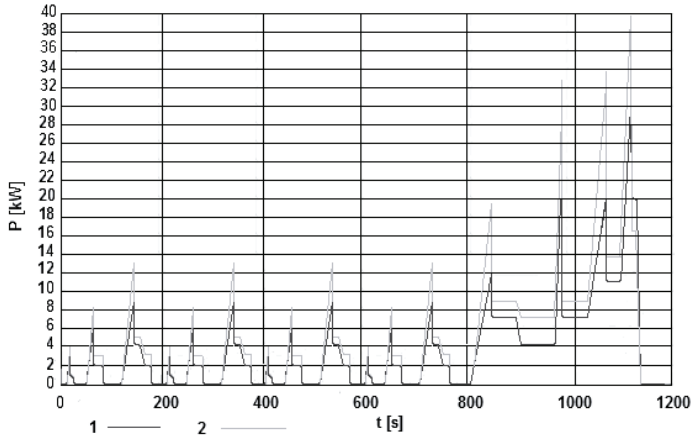

Fig. 8. Engine power P_{ICE} vs. time t; 1 – vehicle with classic combustion engine without trailer, 2 – vehicle with classic combustion engine and with trailer

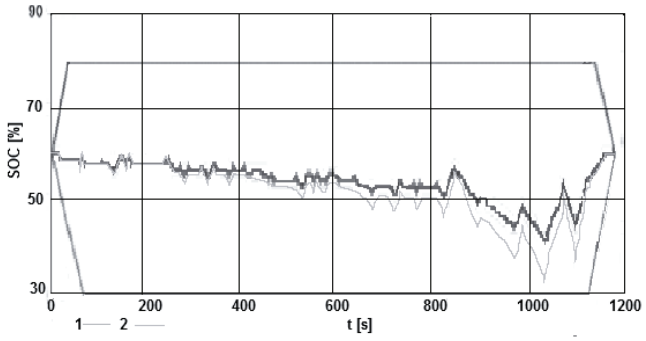

Fig. 9. SOC vs. time t; 1 – hybrid vehicle without trailer, 2 – hybrid vehicle with trailer

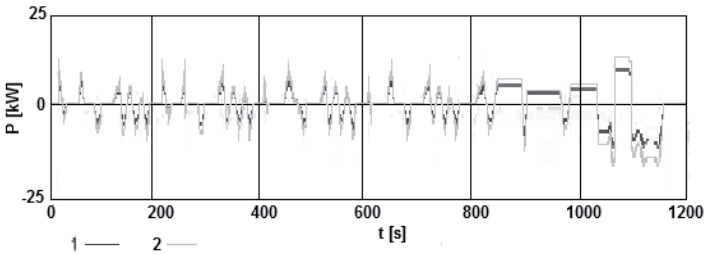

Fig. 10. P_{batt} vs. time t; 1 – hybrid vehicle without trailer, 2 – hybrid vehicle with trailer

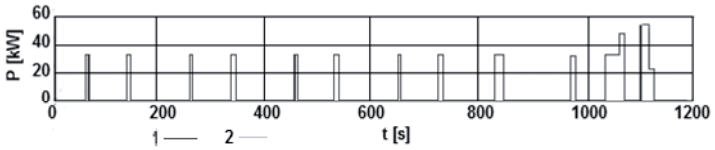

Fig. 11. P_{ICE} vs. time t; 1 – hybrid vehicle without trailer, 2 – hybrid vehicle with trailer

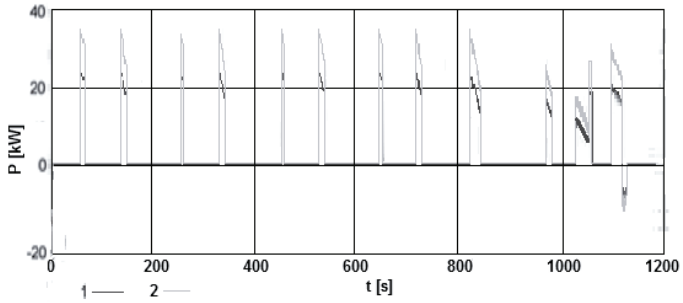

Fig. 12. P_{MG1} vs. time t; 1 – hybrid vehicle without trailer, 2 – hybrid vehicle with trailer

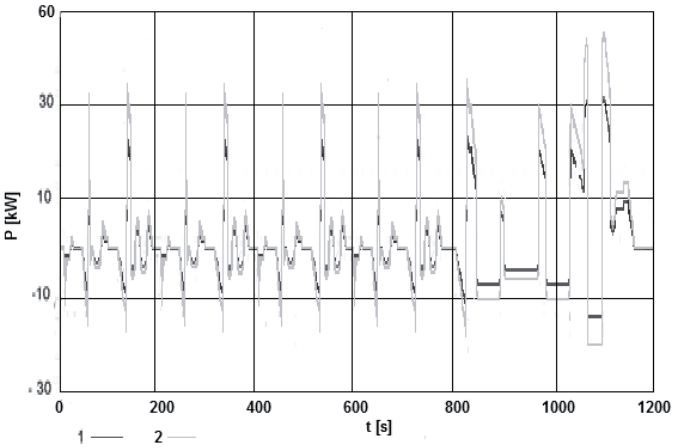

Fig. 13. P_{MG2} vs. time t; 1 – hybrid vehicle without trailer, 2 – hybrid vehicle with trailer

In all cases of vehicle with trailer the powers P_{batt}, P_{MG1}, P_{MG2} have been up 40% higher than in case without trailer.

6. Conclusions

1. In the case of vehicle with classic combustion engine, the operation with trailer need up to 40% power of combustion engine than in case without trailer.
2. In the case of hybrid vehicle, its combustion engine can be operate according its Economic line (e-line), but operation with trailer causes quicker discharging of battery – up to 40%.

References

[1] Mansour, C., Clodic, D., W., *Modeling of the THS-II Series/Parallel Power train and its Energy Management System*, FISITA 2010 World Automotive Congress, Budapest 2010.
[2] Gokce, C., Ustun, O., Yilmaz, M., Tuncay, R. N., *Modeling and Simulation of a Serial – Parallel Hybrid Electrical Vehicle*, http://www.emo.org.tr/ekler/00c3241004b5db7_ek.pdf.
[3] Mansour, C., *Simulation and Validation of Models of Hybrid Vehicles, Case Study of the Toyota Prius*, PhD Thesis MINES ParisTech, Chapter 3, Sep. 2009.
[4] Mansour, C., Clodic, D., W., *Optimized Energy Management Control for the Toyota Hybrid System Using Dynamic Programming on a Predicted Route with Short Computation Time*, International Journal of Automotive Technology February 2012, Vol. 13, Is. 2, pp. 309-324.
[5] Hofman, T., Purnot, T., *Comparative Study and Analysis of an Optimized Control Strategy for the Toyota Hybrid System*, World Electric Vehicle Journal, AVERE, Vol. 3, pp. 1-9, 2009.
[6] Boberg, F., Gustafson, A., *Cost Efficient Hybrid Car-SAAB Automobile*, Lund University, 2007.